Micropatterned Cell–Cell Interactions Enable Functional Encapsulation of Primary Hepatocytes in Hydrogel Microtissues

Citation: Li, Cheri Y., Kelly R. Stevens, Robert E. Schwartz, Brian S. Alejandro, Joanne H. Huang, and Sangeeta N. Bhatia. "Micropatterned Cell–Cell Interactions Enable Functional Encapsulation of Primary Hepatocytes in Hydrogel Microtissues." Tissue Engineering Part A 20, no. 15–16 (August 2014): 2200–2212. © Mary Ann Liebert, Inc.

As Published: http://dx.doi.org/10.1089/ten.TEA.2013.0667

Publisher: Mary Ann Liebert, Inc.

Persistent URL: http://hdl.handle.net/1721.1/99870

Version: Final published version: final published article, as it appeared in a journal, conference proceedings, or other formally published context

TISSUE ENGINEERING: Part A
Volume 20, Numbers 15 and 16, 2014

DOI: 10.1089/ten.tea.2013.0667

Micropatterned Cell–Cell Interactions Enable Functional Encapsulation of Primary Hepatocytes in Hydrogel Microtissues

Cheri Y. Li, PhD,[1] Kelly R. Stevens, PhD,[2] Robert E. Schwartz, PhD,[2] Brian S. Alejandro,[1] Joanne H. Huang, BS,[3] and Sangeeta N. Bhatia, PhD[2,4–7]

Drug-induced liver injury is a major cause of drug development failures and postmarket withdrawals. *In vitro* models that incorporate primary hepatocytes have been shown to be more predictive than model systems which rely on liver microsomes or hepatocellular carcinoma cell lines. Methods to phenotypically stabilize primary hepatocytes *ex vivo* often rely on mimicry of hepatic microenvironmental cues such as cell–cell interactions and cell–matrix interactions. In this work, we sought to incorporate phenotypically stable hepatocytes into three-dimensional (3D) microtissues, which, in turn, could be deployed in drug-screening platforms such as multiwell plates and diverse organ-on-a-chip devices. We first utilize micropatterning on collagen I to specify cell–cell interactions in two-dimensions, followed by collagenase digestion to produce well-controlled aggregates for 3D encapsulation in polyethylene glycol (PEG) diacrylate. Using this approach, we examined the influence of homotypic hepatocyte interactions and composition of the encapsulating hydrogel, and achieved the maintenance of liver-specific function for over 50 days. Optimally preaggregated structures were subsequently encapsulated using a microfluidic droplet-generator to produce 3D microtissues. Interactions of engineered hepatic microtissues with drugs was characterized by flow cytometry, and yielded both induction of P450 enzymes in response to prototypic small molecules and drug–drug interactions that give rise to hepatotoxicity. Collectively, this study establishes a pipeline for the manufacturing of 3D hepatic microtissues that exhibit stabilized liver-specific functions and can be incorporated into a wide array of emerging drug development platforms.

Introduction

A MAJOR CAUSE of clinical trial failures and postmarket drug withdrawals is unexpected liver toxicity. These failures late in drug development not only impact patient safety but also represent a significant economic loss. *In vitro* cell-based models have the potential to rapidly and cost effectively provide early feedback in the drug development process in order to identify toxic candidates for compound prioritization. However, the capacity of these assays to predict clinical observations depends critically on the functional activities of the cell types used in the model platforms. While hepatocellular carcinoma-derived cell lines grow readily in culture, they are inadequate *in vitro* models for liver drug metabolism due to low cytochrome P450 (CYP450) enzyme activity,[1] unresponsiveness to induction,[2] and reduced sensitivity to hepatotoxins.[3] Thus, primary hepatocytes are the preferred cell-based model for drug development applications, yet these cells typically undergo a rapid loss of differentiated function and viability when cultured *ex vivo*.[4–6] This challenge has led to the development of various approaches to stabilize primary hepatocyte functions by recreating some of the architectural and microenvironmental stimuli that surround hepatocytes *in vivo*, such as providing neighboring cells, extracellular matrix (ECM), and soluble factors.[4,5] In addition to so-called two-dimensional (2D) systems, there are a variety of three-dimensional (3D) manipulations that have also shown promise, including spheroids,[7–9] sandwich gels,[10,11] porous scaffolds,[12,13] or encapsulation in natural or synthetic hydrogels.[14–16] The premise of the present study is that the ideal 3D culture platform for drug studies should be amenable to high-throughput assay development and, therefore, amenable to robust miniaturization.

Departments of [1]Chemical Engineering, [2]Health Sciences and Technology, [3]Biology, and [4]Electrical Engineering and Computer Science, Massachusetts Institute of Technology, Cambridge, Massachusetts.
[5]Broad Institute, Cambridge, Massachusetts.
[6]Department of Medicine, Brigham and Women's Hospital, Boston, Massachusetts.
[7]Howard Hughes Medical Institute, Chevy Chase, Maryland.

Miniaturization of cell-laden hydrogels into < 250 μm units, called microtissues, is a promising approach to tissue engineering that provides several distinct advantages over both scaffold-free 3D culture (i.e., spheroids) and conventional hydrogels: (1) In contrast to spheroids or other scaffold-free systems, the cell-encapsulating hydrogel serves a shear-protective function during perfusion, spinner culture, or general handling.[17–19] (2) The hydrogel also prevents aggregation even during culture in small volumes so that the transport of oxygen and nutrients is not limiting.[17,20] (3) Manipulation of scaffold chemistry enables controlled tuning of mechanics[21] or other aspects of the microenvironment, such as entangled whole ECM proteins,[22] adhesive peptides,[14,23,24] or tethered cell signaling factors.[25,26] Thus, conditions can be adjusted for optimal cell survival and function,[27] creating prestabilized microtissue units for downstream handling. (4) Finally, compared with conventional millimeter-scale hydrogels cultured in well plates, microtissues are modular, offering expanded versatility for experimental manipulation and analysis. For example, we have previously described the continuous microfluidic fabrication of polyethylene glycol (PEG) hydrogel microtissues, and the subsequent use of biochemical encoding to direct the formation of patterned tissues from a collection of individual microtissues.[28] We have also shown that due to their miniaturized format, microtissues are amenable to multiplexed[29] and high-throughput flow analysis,[22] bypassing more time-consuming readouts such as confocal microscopy.[30] While these earlier studies have focused on modeling the diseased state of tumor biology, here we seek to apply microtissues to primary mammalian cells and the area of hepatic tissue engineering. There has also been considerable interest in using microtissues as building blocks for bottom-up assembly of patterned tissues[28,31,32] and packed-reactor-like devices.[33–35] However, these studies have yet to be extended to primary hepatocytes, thus far incorporating only the more easily cultured but phenotypically distorted hepatic cell lines.

Here, we report the fabrication of microtissues comprising primary mammalian hepatocytes that can be mass-produced for drug development applications. To stabilize hepatocyte function post-isolation, we first developed a method to form small (< 10-cell) aggregates by patterning hepatocytes on collagen microislands and then detaching the confluent islands. These micropatterned cell–cell interactions enabled hepatocyte survival in bulk PEG hydrogels without adhesive peptides, as well as in 100 μm microtissues, which were produced en masse by continuous microfluidic droplet-based cell encapsulation. Hepatic microtissues exhibited hepatocellular activity as characterized by albumin production and species-specific induction of CYP450 drug metabolism enzymes. Lastly, leveraging the inducibility of the primary hepatocytes, we demonstrate that hepatic microtissues can be used to detect hepatotoxicity and drug–drug interactions.

Materials and Methods

Plate patterning

Topographically patterned polydimethylsiloxane (PDMS; Dow Corning) masking molds that defined collagen microislands were cast from silicon masters. Standard photolithographic methods were used to fabricate the masters with 50 μm tall raised circular pillars of SU-8 2050 photoresist (Microchem). Intermediate PDMS ''negatives'' were cast from the master and coated with (tridecafluoro-1,1,2,2-tetrahydrooctyl)-1-trichlorosilane (UCT Specialties) for 1 h in a vacuum desiccator. Final PDMS masking molds were then cast from the negatives to again have raised pillars, and cut into appropriate discs to fit into six-well plates.

Ultra-Low attachment six-well plates (Corning) were coated with 0.15 mg/mL Type I collagen (rat tail; BD Biosciences) at 37°C for 1 h. Wells were rinsed with deionized water and dried with nitrogen. PDMS masking molds were carefully placed into each well, using gentle pressure to ensure that all parts of the pattern adhered to the well, and the entire plate was subjected to air plasma treatment (SPI Supplies) for 15 s. Nonpatterned control plates meant to have a homogenous collagen surface coating did not undergo this last step. Masking molds were removed from wells for reuse, and plates were sterilized by 15 min of UV exposure before use.

Cell culture and puck formation

Hepatocytes were isolated from 2- to 3-month-old adult female Lewis rats as previously described.[36] Hepatocyte culture medium consisted of Dulbecco's Modified Eagle Medium (DMEM; Invitrogen) with 10% fetal bovine serum (Invitrogen), 0.5 U/mL insulin (Lilly), 7 ng/mL glucagon (Bedford Laboratories), 7.5 μg/mL hydrocortisone (Sigma), 10 U/mL penicillin (Invitrogen), and 10 mg/mL streptomycin (Invitrogen). J2-3T3 fibroblasts were cultured in DMEM with 10% bovine serum (Invitrogen), 10 U/mL penicillin, and 10 mg/mL streptomycin. mCherry J2-3T3 fibroblasts were generated by ViroMag R/L (Oz Biosciences)-mediated transduction of lentivirus containing mCherry under control of the EF-1 alpha promoter (Promega). Transduced mCherry fibroblasts were subsequently selected by puromycin followed by fluorescence-activated cell sorting. All cells were cultured in a 5% CO_2 humidified incubator at 37°C.

To seed freshly isolated hepatocytes, cells were first pelleted at 50 *g* for 5 min and resuspended in hepatocyte medium without serum at a cell density of 2×10^6 hepatocytes/mL. One milliliter of this suspension was added to each well of a patterned or nonpatterned six-well plate. Hepatocytes were allowed to attach for 2 h to any adhesive regions of the plate in the incubator, with gentle linear shaking every 15 min to re-disperse unattached cells. The progress of seeding was monitored under a microscope. After microislands were seeded to confluence, each well was rinsed twice with 2 mL of medium to remove any remaining unattached cells. Cell number on each island was manually counted at 3 h after initial plating, when cells were firmly attached but individual cell borders could be easily distinguished. For hepatocyte-only pucks, the seeded cells were then cultured in 1 mL of hepatocyte culture medium with serum overnight. To form pucks that contain both hepatocytes and fibroblasts, J2-3T3 cells were then added to each well (0.5×10^6 cells in 1 mL hepatocyte medium) and allowed to seed overnight, with gentle shaking every 15 min for the first 2 h.

Encapsulation in bulk PEG gels

Hepatocytes that had been cultured on patterned or nonpatterned plates for 24 h were detached using 2 mg/mL collagenase (Type IV; Invitrogen) in DMEM. Within 5 min, multicellular pucks lifted from the plate but did not dissociate

into single cells. Pucks or unpatterned cells were diluted in hepatocyte medium, pelleted (50 *g*, 5 min), and then resuspended at an effective cell density, calculated from the number of microislands per well and the number of cells per island, of 8×10^6 cells/mL in PEG prepolymer. The prepolymer solution consisted of 100 mg/mL PEG-diacrylate (20 kDa; Laysan Bio) in heavy DMEM (DMEM adjusted to have a specific gravity of 1.06 by OptiPrep density medium; Sigma) with 1:100 v/v photoinitiator working solution (100 mg/mL Irgacure 2959, Ciba, in *n*-vinyl pyrrolidone; Sigma). The adhesive peptide RGDS was incorporated by also including 10 mM of Acrylate-PEG(3.4 kDa)-RGDS monomers, prepared as previously described,[14] in the prepolymer. For coencapsulation of fibroblasts with hepatocyte pucks, J2-3T3 fibroblasts were detached with 0.25% Trypsin-EDTA (Invitrogen), pelleted, and also resuspended in prepolymer for a final 1:1 ratio of fibroblasts and hepatocytes (8×10^6 fibroblasts and 8×10^6 hepatocytes per mL).

Disc-shaped, or ''bulk'' PEG gels were fabricated using hydrogel polymerization apparatus previously described.[37] Briefly, prepolymer solution containing cells was loaded into a 8.5 mm-diameter, 250 μm-thick silicone spacer, sandwiched between a Teflon base and a glass cover slip, and polymerized by exposure to UV light from a spot curing system with a collimating lens (320–390 nm, 21 mW/cm^2, 12 s; Lumen Dynamics). Each gel was soaked in rinse media (DMEM) for 1 h to remove any un-polymerized components and was subsequently cultured in 0.5 mL of hepatocyte medium. All experiments were performed with quadruplicate gels for each condition.

Microfluidic encapsulation in microtissues

Droplet-based microfluidic encapsulation devices were fabricated as previously described.[28] For microfluidic encapsulation, hepatocyte-only or hepatocyte-fibroblast pucks were lifted using 2 mg/mL collagenase, pelleted (50 *g*, 5 min), and then resuspended at an effective hepatocyte density of 30×10^6 cells/mL in PEG prepolymer. The cell suspension was loaded into a syringe and injected into the device at 200 μL/h. Simultaneously, fluorocarbon oil (Fomblin Y-LVAC; Solvay Solexis) containing 0.5% w/v Krytox 157 FSH surfactant (DuPont) was also injected into the device as an oil phase. At a droplet-generating nozzle, the aqueous cell suspension was broken into 100 μm-diameter droplets of cells and prepolymer in oil, which were then continuously polymerized on chip by exposure to UV light (320–390 nm, 500 mW/cm^2, 0.5 s; Lumen Dynamics) before exiting the device. Microtissues collected from the device were separated from oil and washed on a 70 μm strainer to remove any un-polymerized components. To remove gels that did not contain any cells (due to settling of the pucks during injection), microtissues were centrifuged at 50 *g* for 5 min in a Percoll (Sigma) density medium solution (12.5 μL isotonic 1.12 g/mL density Percoll stock per mL of media). Pelleted microtissues were resuspended in hepatocyte medium and cultured in 40 μm strainer caps (BD Falcon) as inserts for 24-well plates. All experiments were performed with quadruplicate wells for each condition.

Biochemical assays

Supernatant was collected every other day from bulk gels or microtissues. Secreted albumin in the supernatant was quantified by an enzyme-linked immunosorbent assay (ELISA) kit using sheep anti-rat albumin antibodies (Bethyl Labs) and horseradish peroxidase detection (3,3′,5,5′-tetramethylbenzidine; Invitrogen).

For enzyme induction experiments, microtissues were pretreated with inducers for 72 h beginning at 48 h postencapsulation. Stock solutions of inducers were prepared in dimethyl sulfoxide (DMSO) and diluted at 1:1000 for final concentrations of 50 μM omeprazole (Sigma), 25 μM rifampin (Sigma), and 10 μM dexamethasone (Sigma). Phenobarbital (Sigma) was dissolved at 40 mM in deionized water and diluted to a final concentration of 200 μM. Vehicle controls were pretreated with 72 h of either 1:1000 DMSO or 1:200 water.

CYP450 activity was assessed with luminogenic P450-Glo™ CYP450 assay kits (Promega) according to vendor instructions for nonlytic assays using cultured cells. Microtissues were incubated with Luciferin-PFBE (1:40 dilution in phenol-free DMEM), Luciferin-CEE (CYP1A1, 1:66 dilution), or Luciferin-H (CYP2C9, 1:50 dilution) for 3 h. Processed medium samples from each strainer of microtissues were collected, and luciferin metabolites were measured on a luminometer (10 s; Berthold).

Acetaminophen treatment

For hepatotoxicity experiments, microtissues were cultured for 72 h postencapsulation and then exposed to 0–40 mM of acetaminophen (Sigma) for 24 h. All samples contained a final 0.8% v/v DMSO. For drug interaction experiments, microtissues were cultured for 48 h postencapsulation, exposed to various inducers or controls for 72 h, and then dosed with 40 mM of acetaminophen in the presence of inducers for 24 h.

Large-particle flow cytometry

A high-throughput analysis of microtissue viability was performed by first staining microtissues in suspension with the live-dead fluorescent stains calcein AM (5 μg/mL) and ethidium homodimer (2.5 μg/mL) for 15 min at 37°C. Whole-microtissue levels of fluorescence were detected using a BioSort large particle flow cytometry (Union Biometrica) that was equipped with a 488 nm excitation laser. Microtissues were gated for on the basis of Time of Flight (size) and Extinction (optical density) to exclude debris. Fluorescent signal acquisition parameters were set as follows: Gains—Green 3, Red 3, PMT control—Green 300, Red 700. Compensation was applied to subtract 90% of the green signal from red. Scatter plots were created using BioSorter software. Raw data were also exported for processing with a custom MATLAB code.

Immunohistochemistry, live-dead staining, and imaging

For immunohistochemistry, fresh isolated hepatocytes or hepatocyte microtissues were fixed in methanol and 10% acetic acid and then gently pelleted in eppendorf tubes. Cell pellets were resuspended in histogel (Thermo Scientific), repelleted, and placed on ice for histogel gelation. Histogel-encapsulated cell pellets were processed, embedded, and sectioned. Sections were incubated with primary antibodies against either pan-cytokeratin (1:800; Sigma) or arginase-1 (1:400; Sigma) and then with species-appropriate secondary

antibodies conjugated to Alexa 488 or 555. Images were obtained using a Nikon Ti scanning-confocal microscope.

Cell viability within bulk gels and microtissues was examined using calcein AM (5 μg/mL) and ethidium homodimer (2.5 μg/mL) fluorescent stains (Molecular Probes; incubated with cells for 15 min at 37°C) to stain live and dead cells, respectively. Images were acquired using a Nikon Ellipse TE200 inverted fluorescence microscope and CoolSnap-HQ Digital CCD Camera. MetaMorph Image Analysis Software was used to uniformly adjust brightness/contrast, pseudocolor, and merge images.

Results

Control and uniformity of hepatocyte patterning

Both homotypic and heterotypic cell–cell interactions have been reported to modulate the function of primary hepatocytes in patterned 2D culture[38–40] as well as in various 3D culture systems.[14,15,41] Based on these reports, we hypothesized that in order to establish a microtissue system that supports functional primary hepatocytes, it would be critical to facilitate physical cell–cell contacts. Thus, we chose to preaggregate hepatocytes into small (< 100 μm) multicellular units before 3D encapsulation of the cells. Furthermore, we sought to do so in a manner that could produce units with narrow-sized dispersity for downstream microfluidic processing (i.e., for consistent flow), and was easily scalable to millions of aggregates. We investigated an approach in which hepatocytes were seeded into clusters on 2D micropatterns, allowed to form cell–cell contacts, and then detached as aggregates. To direct cell seeding, collagen micro-islands were patterned on tissue culture plates using a soft lithography process[39] in which a layer of adsorbed collagen is masked by contact with a PDMS mold (Fig. 1a).

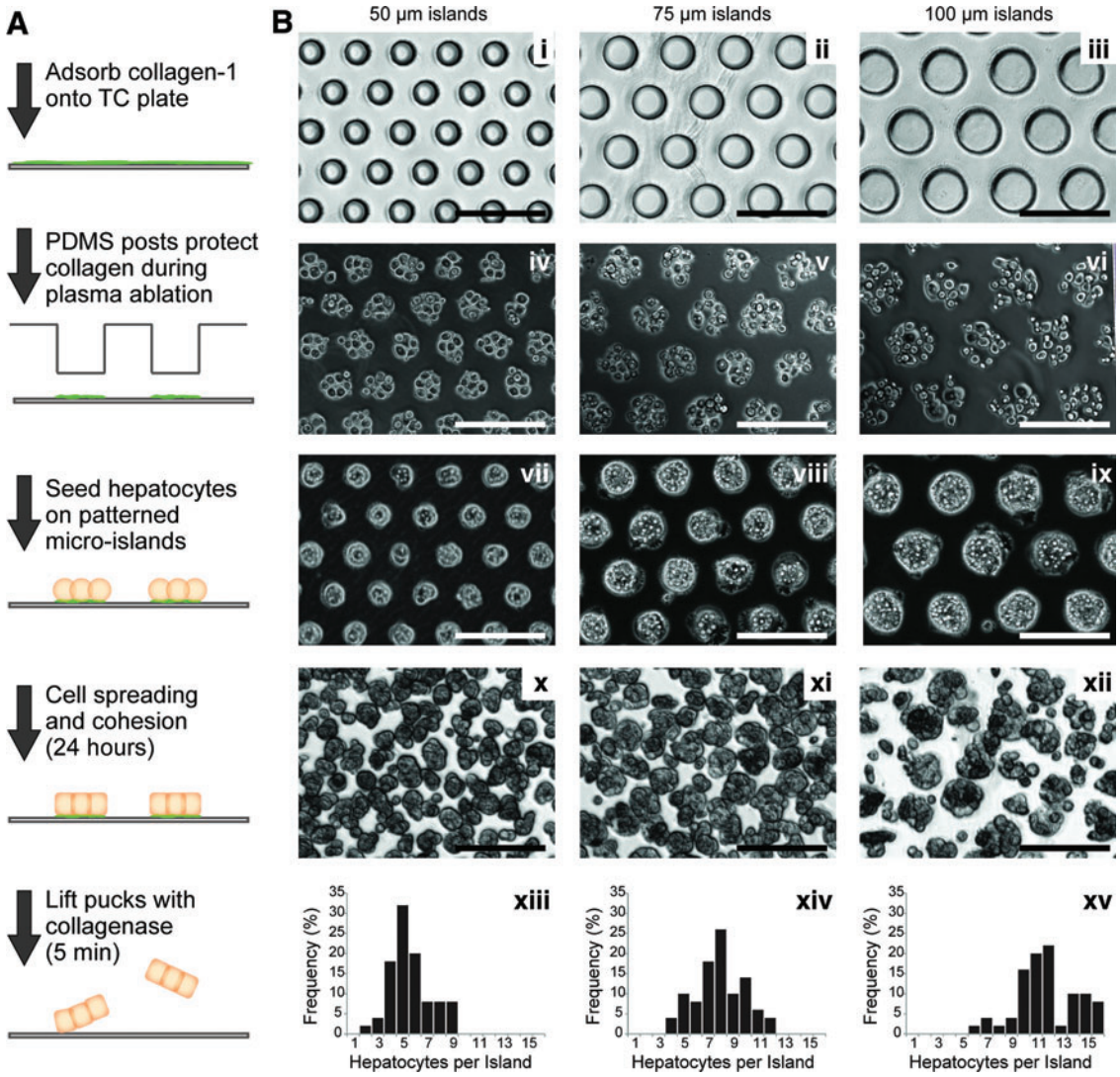

FIG. 1. Hepatocyte puck formation and detachment from patterned collagen microislands. **(A)** Schematic representation illustrating the definition of adhesive collagen islands on plastic, hepatocyte seeding and spreading over 24 h, and detachment with collagenase. **(B)** Phase images showing **(i–iii)** polydimethylsiloxane (PDMS) molds to define island size, **(iv–vi)** primary rat hepatocytes initially seeded on the islands, **(vii–ix)** confluent hepatocyte islands after 24 h of culture, and **(x–xii)** detached pucks. All scale bars are 200 μm. **(xii–xv)** Histogram of number of the hepatocytes in each size of puck as counted 3 h postseeding. Color images available online at www.liebertpub.com/tea

Protruding PDMS posts of various sizes (50, 75, and 100 μm diameters) (Fig. 1b, i–iii) were used to protect collagen in contacted regions from plasma ablation, resulting in 50–100 μm circles of remaining collagen. This range of island sizes was selected to be compatible with subsequent encapsulation in hydrogels as small as 100 μm in diameter. Freshly isolated primary hepatocytes were then seeded onto micropatterned collagen islands of various sizes (50, 75, and 100 μm diameters). Hepatocytes densely covered and adhered only to the areas of collagen microislands (Fig. 1b, iv–vi). This patterning process was robust and scalable to large areas (Supplementary Fig. S1; Supplementary Data are available online at www.liebertpub.com/tea), which enabled mass production of patterned hepatocyte clusters.

After one day of culture, (Fig. 1b, vii–ix), hepatocytes spread to form a confluent 2D layer over each microisland. When treated with collagenase to digest underlying collagen, the small circles of hepatocytes, or hepatocyte ''pucks,'' detached from the plate as cohesive units (Fig. 1b, x–xii) without dissociating into single cells, presumably due to minimal digestion of cell surface proteins by collagenase. Cell number in each puck, counted manually after attachment but before cell spreading, was directly related to island area and generally followed the Poisson distribution (Fig. 1b, xiii–x; 5.6 ± 1.7 cells for 50 μm islands, 7.9 ± 2.0 cells for 75 μm islands, and 11.8 ± 2.4 cells for 100 μm islands). Since even smaller island sizes led to many islands only capturing single cells, all subsequent studies used pucks formed by 50 μm islands. After removal from the collagen substrate, hepatocytes in freely floating pucks expressed both cytokeratin and arginase-1 (Supplementary Fig. S2), indicating that puck culture enabled the selection for viable hepatocytes after fresh isolation procedures. Taken together, these results show the advantages of controlled, 2D micropatterning, which prompts robust and effective formation of cell–cell contacts.

Effect of homotypic contacts on 3D albumin secretion

To examine whether preaggregation of hepatocytes into pucks improved hepatic function after encapsulation in a 3D hydrogel, we measured the albumin secretion of the cells within monolithic, ''bulk'' PEG gels as a gauge of hepatic phenotype and viability. For the hydrogel scaffold material, 10% w/w PEG diacrylate (PEG-DA, 20 kDa) was chosen, because it is (1) permeable enough to enable the diffusion of oxygen/nutrients/proteins to and from the cells,[42] (2) biologically/immunologically inert, and (3) can be functionalized with acrylate-containing ligands.[23,43,44] As a control condition, hepatocytes were randomly seeded in collagen-coated but unpatterned six-well plates at 600,000 cells/well, which was chosen to match the theoretical number of cells that would seed in a 50 μm-island patterned well assuming 5.6 hepatocytes per island. At this density, cells on the unpatterned surfaces are able to make chance cell contacts, as they seed in 2D and form loose cords of cells when detached (Fig. 2a, b). Hepatocytes were randomly seeded (''unpatterned'') or micropatterned using collagen islands for 24 h, lifted by collagenase, resuspended in hydrogel prepolymer, and photopolymerized into 14 μL disc-shaped gels (Fig. 2c). Live/dead staining with calcein AM and ethidium homodimer on the encapsulated pucks showed $>80\%$ viability after 3 h (Fig. 2d), indicating that the polymerization process itself was not additionally cytotoxic relative to the viability of hepatocyte pucks after detachment but before encapsulation ($\sim 80\%$). Hydrogels containing hepatocyte pucks exhibited increasing albumin secretion during the first week after encapsulation followed by sustained secretion for approximately 2 weeks (Fig. 2e). Albumin secretion in hydrogels containing pucks was more than three-fold greater compared with control hydrogels containing unpatterned hepatocytes at 8 days ($p = 0.0571$, $n = 4$, Wilcoxon rank sum test). These results demonstrate that micropatterning hepatocytes to form hepatic pucks before encapsulation improves hepatocyte phenotype after encapsulation in a 3D hydrogel.

Effect of other supporting factors in 3D albumin secretion

Co-culture of hepatocytes with a second cell type,[39,41] or the presence of adhesion proteins or peptides such as RGDS,[14,15] have been previously reported to support the maintenance of primary hepatocyte function. Thus, we explored the incorporation of heterotypic cell–cell interactions and ECM-derived adhesive moieties into the 3D gels (Fig. 2f). To achieve the former, a single-cell suspension of J2-3T3 fibroblasts expressing constitutively fluorescent mCherry was mixed into the prepolymer used to encapsulate hepatocyte pucks. Resultant gels (Fig. 2g) contained J2-3T3 fibroblasts (shown in blue) distributed throughout the volume of the gel, at length scales that previous studies have demonstrated to enable paracrine signaling through soluble factors[38] (<100 μm from the nearest hepatocyte) as well as, in some cases, immediately adjacent to hepatocytes. Adhesive moieties were incorporated into gels by chemically conjugating acrylate-functionalized RGDS peptides (10 mM) into the hydrogel network. A 3D co-culture of fibroblasts with hepatocyte pucks resulted in a greater than two-fold increase of albumin production relative to hepatocyte-only controls in the first week (Fig. 2h). More importantly, the maintenance of albumin production over time was extended in the presence of fibroblasts from 20 days to more than 7 weeks. Conversely, in RGDS-containing gels compared with nonadhesive controls, adhesive peptides did not significantly affect albumin production curves whether the gels contained hepatocyte pucks only or hepatocyte pucks with fibroblasts (Fig. 2h). Together, these results show that supportive cues from J2-3T3 fibroblasts but not RGDS-adhesive peptides are crucial for long-term hepatocyte survival in this system.

Microfluidic production of primary hepatic microtissues

As shown earlier, hepatocyte pucks retain function when encapsulated with fibroblasts in macroscopic bulk PEG hydrogel. Thus, we sought to miniaturize the 3D-engineered tissue into 100 μm-diameter ''microtissues.'' We produced individual droplets of prepolymer containing cells and then polymerized these cellular droplets to form ''microtissue'' hydrogels on-chip (Fig. 3a). Hepatocyte pucks, fibroblasts, and photopolymerizable prepolymer were mixed to form a combined aqueous stream that was injected into the encapsulation device. This aqueous stream was designed to intersect with an oil stream of oxygen-permeable fluorocarbon oil at a droplet-generating nozzle, such that prepolymer-in-oil droplets were continuously produced. Droplets subsequently passed under a UV light source and were polymerized within

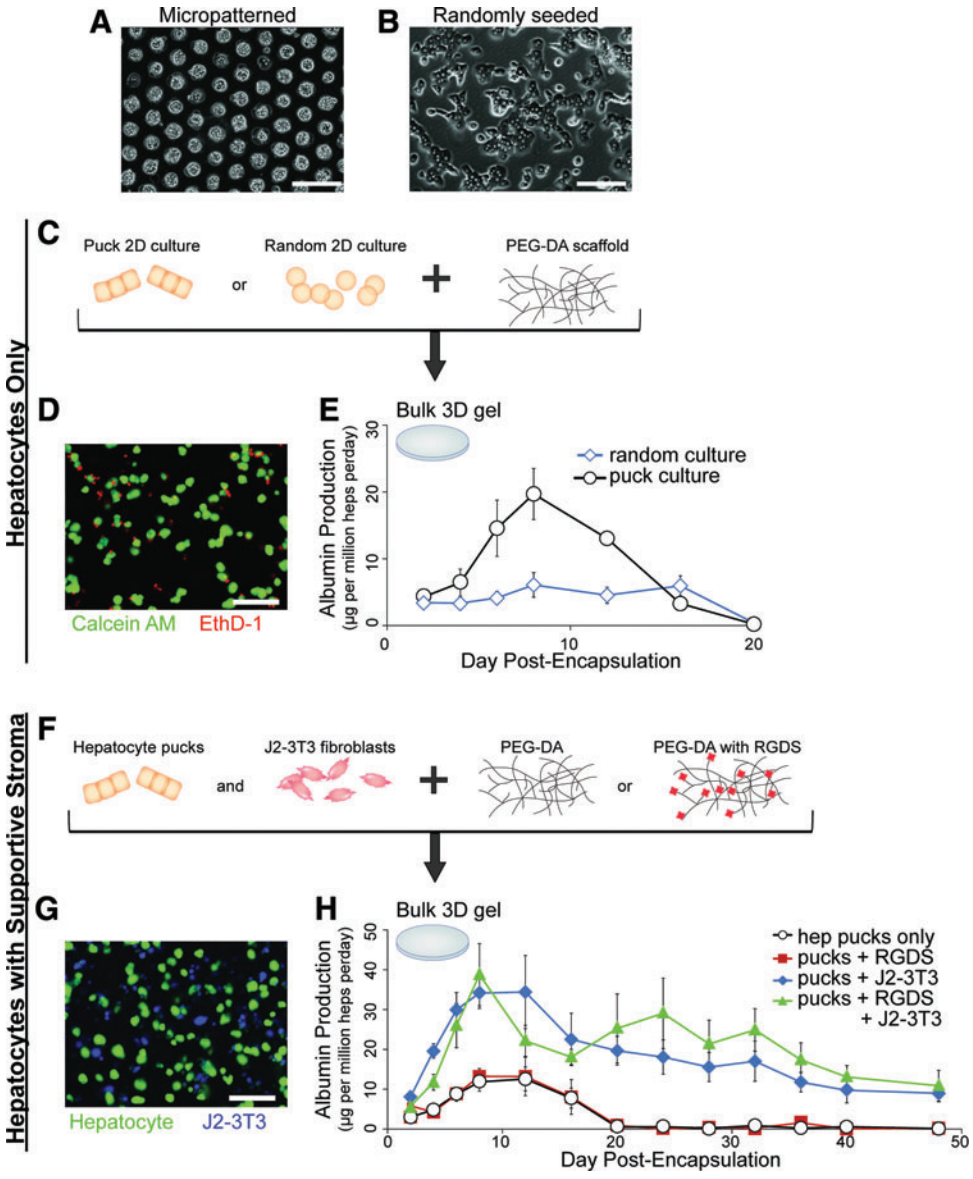

FIG. 2. Homotypic and heterotypic cell–cell interactions increase albumin secretion by hepatocytes in 8.5-mm-diameter bulk polyethylene glycol (PEG) hydrogels. Hepatocytes were cultured in 2D on either **(A)** micropatterned islands or **(B)** unpatterned collagen-coated plates. **(C)** Hepatocytes were detached from each 2D culture format after 24 h and encapsulated in a 3D PEG scaffold. **(D)** Hepatocytes pucks are viable within the hydrogel as visualized by a live-dead stain. **(E)** Hepatocyte-laden gels containing pucks secrete more albumin, quantified by ELISA, into the supernatant than gels containing unpatterned hepatocytes ($n = 4$). **(F)** J2-3T3 fibroblasts were coencapsulated along with hepatocytes into the hydrogel, which was modified by RGDS adhesive peptides. **(G)** Epifluorescence image of hepatocyte pucks (green, calcein) and fibroblasts (blue, mCherry) coculture within a gel. **(H)** The addition of fibroblasts to gels containing hepatocyte pucks increases the amount and longevity of albumin secretion. Incorporated RGDS does not have a significant effect ($n = 4$). Error bars show standard error (SEM). All scale bars are 200 μm. Color images available online at www.liebertpub.com/tea

the device (Fig. 3b and Supplementary Video S1). Although both microtissues and bulk gels were photopolymerized from the same prepolymer composition, the continuous fabrication of microtissues necessitated much higher light intensities (500 mW/cm^2 instead of 21 mW/cm^2) but with only a short exposure time of 0.5 s. Polymerized, spherical microtissues containing multicellular pucks were collected from the outlet of the chip. Viability of primary hepatic microtissues as assessed by live-dead staining was similar to that of bulk-encapsulated pucks (Fig. 3c). Consistent with the results observed using bulk hydrogels, the presence of dispersed fibroblasts mixed into the gels significantly increased total albumin produced over 16 days (Fig. 3d).

After establishing that fibroblasts play a key supportive role in maintaining hepatocyte puck function, we explored the impact of providing this heterotypic interaction earlier in the process, during the first 24 h posthepatocyte isolation. A previous study in 2D has shown that early physical cell–cell contact with fibroblasts, especially in the first 18 h postisolation, was critical to hepatocyte function compared with if the hepatocytes received soluble signals from fibroblasts but were physically isolated.[38] To include fibroblasts when hepatocytes are stabilizing in 2D, fibroblasts were seeded onto any remaining space on the microislands after hepatocytes had been allowed to attach for 2 h. When unattached fibroblasts are rinsed off after 2 more hours, 95% of the resulting islands contained both cell types (Fig. 3e and Supplementary Fig. S3), and as earlier, formed confluent circles of cells over 24 h that could be discretely detached by collagenase to produce mixed hepatocyte-fibroblast pucks. Thus, by patterning co-culture pucks, we introduce supportive fibroblasts earlier and in a closer configuration (contact vs. paracrine), the latter of which has been shown to improve *in vivo* long-term hepatocyte function in scaled-up, patterned implants.[45] We further ensure that the two cell types do not separate during microfluidic injection due to size and density differences. Compared with randomly seeded hepatocytes where some cells may form large multi-cellular clusters while others remain individual, the use of prepatterned mixed pucks

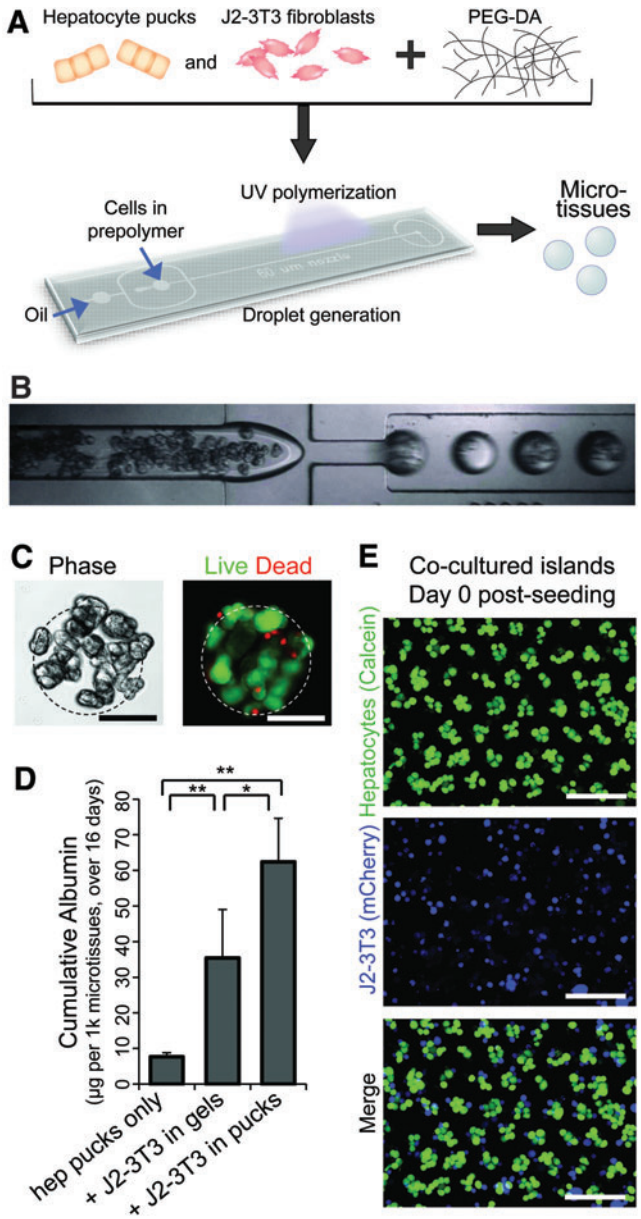

FIG. 3. Microfluidic encapsulation of hepatocyte pucks. **(A)** A mixture of hepatocyte pucks and fibroblasts are encapsulated using a **(B)** microfluidic droplet generating device to polymerize ~100 μm-diameter spherical cell-laden hydrogels. Scale bar = 200 μm. **(C)** Phase image and viability staining of an individual microtissue containing several hepatocyte-only pucks. The dotted line indicates the edge of the hydrogel. Scale bar = 50 μm. **(D)** Microtissues containing hepatocyte-fibroblast mixed pucks secrete more cumulative albumin over 16 days than microtissues containing either hepatocyte pucks only, or hepatocyte pucks with a single-cell suspension of fibroblasts. Error bars show standard error (SEM). $n = 4$ wells, $^{*}p = 0.0571$, $^{**}p = 0.0286$, Wilcoxon rank sum test for pairwise comparisons. **(E)** Hepatocytes and fibroblasts seeded together onto micropatterned islands to form co-cultured pucks. Fluorescent images of the two cell types right after seeding showing the distribution of fibroblasts onto each island. Scale bars = 200 μm. Color images available online at www.liebertpub.com/tea

decreases the size variance of objects entering the microfluidic encapsulation device, thus improving the reliability and consistency of microtissue fabrication, while incorporating a greater majority of hepatocytes in stabilized aggregates. Microtissues containing hepatocyte-fibroblast pucks, where the two cell types were brought into contact on the day of hepatocyte isolation, displayed the most optimal hepatic function as measured by total amounts of secreted albumin, producing 70% more than microtissues containing hepatocyte pucks and fibroblasts mixed 24-h postisolation (Fig. 3d), and, thus, were chosen for use in all subsequent studies.

Characterization of microtissue drug metabolism enzyme activity

Of the many metabolic functions that hepatocytes perform in the body, xenobiotic detoxification is essential in an *in vitro* model used for drug development. Microsomes, which are vesicle-like structures reformed from fragments of endoplasmic reticulum from homogenized hepatocytes, are commonly used in high-throughput systems to identify enzymes involved in drug metabolism, but lack the dynamic gene expression and intact cellular machinery required for toxicity testing. For the prediction of single- or multi-drug toxicity, cell-based models are desirable, because nuclear receptors in hepatocytes modulate levels of enzyme activities and drug interactions. We characterized the liver-specific drug metabolism functions of primary hepatic microtissues by assessing their CYP450 enzyme activity in response to known pharmacological inducers. Microtissues were dosed with inducers omeprazole (50 μM), dexamethasone (10 μM), rifampin (25 μM), or phenobarbital (200 μM) at 2 days after encapsulation. After a 72 h incubation period, the activity of several CYP isozymes was quantified using a luminogenic CYP450 assay. We observed levels of CYP function induction that correlated well with the literature: a nine-fold increase in CYP1A1 activity by omeprazole, a seven-fold increase in CYP3A4 activity by dexamethasone, a two-fold increase in CYP2C9 activity by rifampin, and a two-fold increase in CYP3A4 activity by phenobarbital (Fig. 4).[46–49]

Microtissue platform to detect hepatotoxicity and drug–drug interactions

To assess the suitability of primary hepatic microtissues for 3D drug toxicity studies, we treated microtissues with varying concentrations of the common analgesic, acetaminophen (APAP). Acetaminophen itself is nontoxic until it is metabolized by P450 enzymes in primary hepatocytes, including CYP3A4, CYP2E1, and CYP1A2,[50] into the reactive metabolite N-acetyl-p-benzoquinone imine (NAPQI). Due to their reduced P450 activity, immortalized hepatocyte cell lines are often highly resistant to acetaminophen hepatotoxicity.[51] We treated primary hepatic microtissues with acetaminophen for 24 h, and then co-stained microtissues using calcein AM (live) and ethidium homodimer (dead). The miniaturized 3D format of the microtissues enabled the use of a large-particle flow cytometer for high-throughput detection of individual microtissue viability in each treatment group (Fig. 5a). Overall levels of live (green) and dead (red) staining were measured for each microtissue in control or APAP-exposed populations. At lower concentrations of acetaminophen (0–15 mM), the microtissue population was

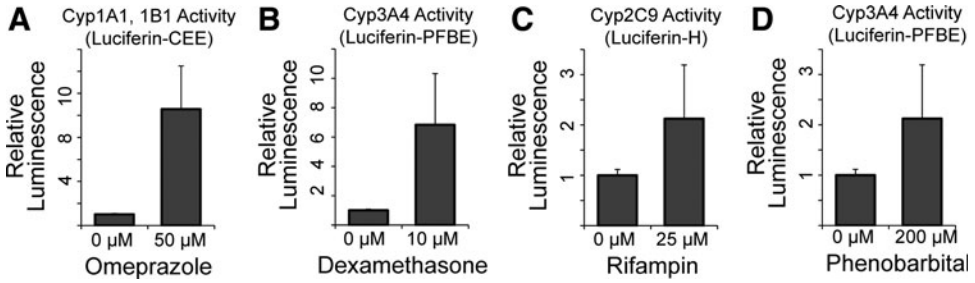

FIG. 4. Induction of cytochrome P450 (CYP450) activity in primary hepatocyte/fibroblast microtissues. Microtissues were exposed to inducers for 72 h before measurement of CYP450 activity using luminogenic substrates. **(A)** CYP1A1 activity induced by 50 μM omeprazole. **(B)** CYP3A4 activity induced by 10 μM dexamethasone. **(C)** CYP2C9 activity induced by 25 μM rifampin. **(D)** CYP3A4 activity induced by 200 μM phenobarbital. Luminescent signals were scaled relative to uninduced vehicle controls, all groups were $n = 3$ wells, with 100,000 microencapsulated hepatocytes per well. Error bars show standard error (SEM).

detected with generally high green (live) fluorescence and low red (dead) fluorescence, as represented on a scatter plot (Fig. 5b). However, after the treatment of microtissues with 40 mM APAP, the fluorescent signals of the population shifted downward (less green) and to the right (more red), indicating a range of degrees of cell death per microtissue within the pool of treated microtissues. By gating to separate fully viable microtissues from those with some level of reduced viability (Fig. 5c), we quantified the proportion of viable microtissues when treated with increasing APAP doses and observed a nonlinear toxicity ''shoulder'' below which there was little effect, but above which hepatotoxicity is observed. The shape of this dose curve may be attributed to the depletion of intracellular glutathione[52] and has been observed in other primary hepatocyte systems,[39,53] indicating that these microtissues faithfully detect a canonical example of primary hepatocyte toxicity.

We next sought to explore whether the primary hepatic microtissue-based toxicity platform could detect canonical hepatocyte-mediated drug–drug interactions, in which induction of a CYP450 enzyme by exposure to one drug leads to more rapid metabolism of a subsequently dosed drug, affecting its toxicity or efficacy. Since we demonstrated that hepatic microtissues are responsive to CYP450 induction, we subjected them to co-treatment with (1) a pharmacologic inducer (omeprazole, dexamethasone, rifampin, or phenobarbital) and (2) acetaminophen. Preincubation of microtissues with omeprazole, which is reported to induce CYP1A2,[54] before treatment with acetaminophen increased the amount of dead staining and decreased the amount of live staining compared with acetaminophen-only treated microtissues (Fig. 6a) as analyzed by large-particle flow cytometry. Pretreatment with dexamethasone, which is known to induce CYP3A4 activity[47] (Fig. 4b), also exacerbated acetaminophen-induced hepatotoxicity (Fig. 6b). Conversely, rifampin and phenobarbital, which are poor inducers of rat CYP3A4,[47,48] did not significantly increase acetaminophen toxicity (Fig. 6c, d). Together, these data indicate the ability of hepatic microtissues to integrate responses to multiple drugs and to detect cytochrome-P450-mediated drug interactions.

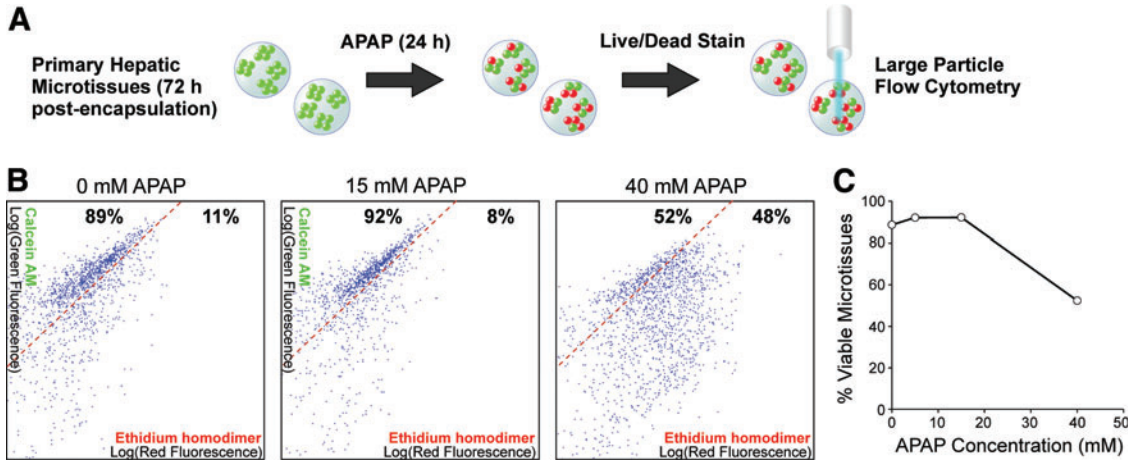

FIG. 5. Microtissues are susceptible to acetaminophen-elicited hepatotoxicity. **(A)** Live-dead staining and large particle flow cytometry were used to detect level of toxicity on a per-microtissue basis. **(B)** Scatter plots of microtissue fluorescence (green—live, red—dead) after 24 h incubation with various doses of acetaminophen. Upper left gate set based on repeated control conditions indicates% of all microtissues in the population that do not show reduced cell viabilities (% viable microtissues). **(C)** Cliff-point for APAP toxicity observed in % viable microtissue dose curve. $n > 1000$ microtissues in each population. APAP, acetaminophen. Color images available online at www.liebertpub.com/tea

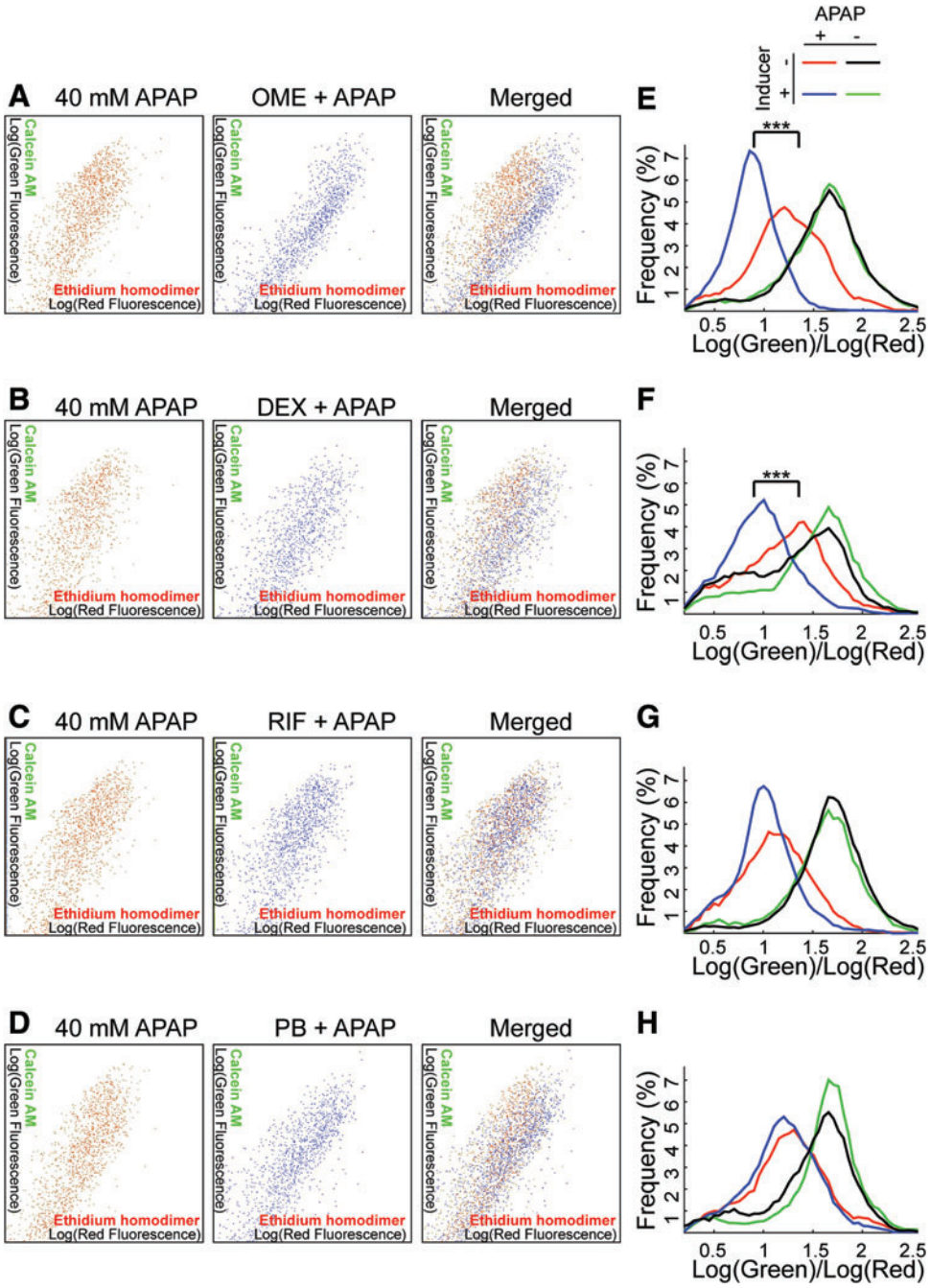

FIG. 6. Hepatic microtissues detect CYP450 inducer interactions with acetaminophen toxicity. **(A–D)** Flow cytometry scatter plots of microtissues treated with 40 mM APAP after 72 h of induction with **(A)** 50 μM omeprazole, **(B)** 10 μM dexamethasone, **(C)** 25 μM rifampin, or **(D)** 200 μM phenobarbital. Green—calcein, live. Red—ethidium homodimer, dead. Omeprazole and dexamethasone exacerbate acetaminophen toxicity. **(E–H)** Histogram representation of microtissue populations, quantifying ratio of green versus red signal with higher ratios indicating a higher percent of viable cells in the microtissues. Treatment and control groups are coded as follows − orange: APAP only, blue: inducer + APAP, green: inducer only, black: vehicle control. $n > 1000$ microtissues in each population, *** indicates p-value $< 10^{-4}$ (one-way analysis of variance, Tukey *post-hoc* test). Color images available online at www.liebertpub.com/tea

Discussion

Cell-based *in vitro* systems capable of modeling the response of *in vivo* liver tissue to toxic insults could help reduce the number of late-stage drug development failures, but require the optimization of *in vitro* culture for primary hepatocytes. In this study, we developed a modular method that maintains hepatocyte function using established 2D culture paradigms to induce preaggregation of primary hepatocytes before 3D encapsulation. Using an array of microfabrication and microfluidic techniques, we have, for the first time to our knowledge, encapsulated primary hepatocytes within PEG microtissues. The initial prepatterning step stabilized cell–cell contacts and enabled hepatocyte function for more than 50 days. The resulting 3D-encapsulated PEG microtissues, which exhibit inducible CYP450 activity and can detect hepatotoxic drugs and combinations, offer suitability for high-throughput studies of primary hepatocytes.

Conventional techniques used to form 3D aggregates, such as culturing cells in rotational suspension,[20,55] or on nonadhesive plates,[56] can take multiple days to incorporate all cells, and lead to spheroids that are nonuniform in shape and size.[20,57,58] To address this problem, various microtechnology-based methods to enhance spheroid uniformity have been developed,[58] including hanging-drop platforms[59] or centrifugation into microwells,[60] but remain limited with regard to expense and throughput. In this

study, we have described a novel ''2D to 3D'' fabrication method to produce such aggregates by seeding cells on large arrays of $< 100\,\mu m$ micropatterned collagen islands, and detaching intact cell aggregates from each island with collagenase (Fig. 1). Compared with the use of thermally responsive coatings for cell-sheet-to-spheroid formation, which requires specialty chemical functionalization that is not widely accessible,[61] our collagen-patterned method is simpler and more scalable especially for small aggregates. The ability to easily define a range of uniform island sizes, and hence the number of cells per aggregate and the size of the detached pucks, illustrates that control can be achieved over puck characteristics and homogeneity. In contrast to other 3D aggregation methods, our protocol, in addition, selects only adhesive hepatocytes from the freshly isolated population of primary cells, thus filtering out any nonviable cells. Most importantly, our method is orders of magnitude higher in throughput compared with hanging drop (96 or 384 spheroids/plate) or microwell plates (28000 spheroids/plate), especially for small aggregates. Using our method, one six-well plate patterned with $50\,\mu m$ islands can template more than 600,000 pucks, or $\sim 3 \times 10^6$ hepatocytes assuming five hepatocytes per puck.

By examining the function of primary rat hepatocyte pucks encapsulated in macroscopic PEG hydrogels, we found that preaggregation of the hepatocytes increased the levels of albumin secreted from cell-laden hydrogels (Fig. 2c), which is consistent with literature reports on the effects of homotypic hepatocyte interactions.[4] The addition of co-encapsulated J2-3T3 fibroblasts into the hydrogels improved hepatocyte performance even more, corroborating the phenotypic advantage gained from co-culture reported in other culture formats (Fig. 2f).[4,39–41] Notably, further functionalizing the PEG hydrogel with adhesive RGDS peptides did not have a significant effect on albumin production by encapsulated hepatocytes. Integrin ligation by RGDS has been reported to confer survival to isolated hepatocytes through the Akt pathway.[62] In addition, although cellular response to RGD can depend on how the peptide is presented (e.g., clustering density[63]), we have conjugated RGDS to 10% PEG-DA hepatocyte-laden hydrogels using the same co-polymerization route in the past.[15] That RGDS was not necessary for optimal hepatocyte function in the present case may be due to cross-talk between cell–matrix and cell–cell interaction pathways,[64–66] and suggests that cell–cell contacts established during the 2D phase of microtissue construction were sufficient to alleviate the need for any cell–matrix contacts in 3D, as the PEG hydrogel background is biologically inert. Alternatively, it is possible that despite collagenase digestion, secreted ECM molecules remain attached to hepatocytes and are subsequently immobilized during encapsulation.[67]

We have evaluated the function of primary hepatocytes within PEG microtissues over several weeks, including prolonged albumin secretion, and maintained the activity of several major CYP450 isozymes: CYP1A1, CYP3A4, and CYP2C9 (Fig. 4). Moreover, we have demonstrated the induction of metabolic activity in response to omeprazole, dexamethasone, rifampin, and phenobarbital. Given these intact drug metabolism characteristics, the miniaturized 3D format of microtissue culture enables high-throughput toxicity and drug–drug interaction screens. *In vivo* studies that assess large numbers of compounds can be slow, expensive, and require significant compound scale-up for dosing. Advantages of the microtissue system for such toxicity screening include being amenable to fast flow cytometry-like fluorimetric readouts that provide population data. In contrast to spheroid cultures, where uncontrolled aggregation often results in large spheroids with necrotic cores,[4,9,17,20] hepatic microtissues are protected from both shear and aggregation, and can be cultured in small volumes without such consequences. Thus, experiments can be designed with large numbers of replicate microtissues to acheive statistical power while still minimizing the amounts required of early development compounds, which can be limiting. Furthermore, unlike monolithic 3D tissues, our primary hepatic microtissues are modular and can be integrated with a variety of different experimental platforms. Here, we not only cultured microtissues in a static media on a porous support, but they could also, for example, be cultured in mixed suspension or microfluidically perfused. Finally, microtissues containing different types of cells could be easily combined to explore signaling or metabolite interactions between tissues.

To illustrate the potential of primary hepatic microtissue-based drug toxicity screening, we performed a dosing experiment with the hepatotoxic drug acetaminophen (Fig. 5). Compared with pooled biochemical assays such as MTT assays on 2D hepatocytes,[39] these data offer insights into not only the average degree of hepatotoxicity observed, but also the range of responses across the microtissue population (Fig. 5b). We have also completed a 6-day drug–drug interaction experiment (Fig. 6). Combined, these results suggest the utility of this system for screening new drug candidates, with the potential for longer treatment times and complex dosing schemes (multiple doses, drug co-treatment) that cannot be performed in short-lived liver slices or microsomes. Future work will incorporate automated liquid handling and more specialized fluorescent indicators of hepatocyte injury.[68]

Throughout this study, primary rat hepatocytes were used to establish patterning and encapsulation techniques. We and others have previously found that the qualitative rules developed to culture primary hepatocytes often translate cross-species from rat to human hepatocytes.[4,14,15,39,45,69] Therefore, we anticipate that these methods will be extendable to primary human hepatocytes in future iterations of our platform. It is notable that the resulting hepatic microtissues described here accurately reflect their species-specific origin. Specifically, microtissues displayed a seven-fold induction of CYP3A4 by dexamethasone, which is comparable to the fold inductions reported for rat hepatocytes (approximately three to eight-fold from various donors, while no induction was observed for human hepatocytes[47]). Accordingly, dexamethasone induction increased hepatotoxicity from acetaminophen exposure (Fig. 6b), which is known to be metabolized through CYP3A4. Phenobarbital and rifampin, in contrast, are strong CYP3A4 inducers in primary human hepatocytes but less so for rat hepatocytes,[48] consistent with our finding that phenobarbital led to only a 2-fold induction of CYP3A4 in microtissues (Fig. 4d). Thus, as expected, phenobarbital and rifampin did not significantly affect acetaminophen hepatotoxicity (Fig. 6c, d). Therefore, although the hepatic microtissues

characterized here may not be directly predictive of human clinical outcomes, these results suggest that microtissues derived from human hepatocytes may display human-specific induction patterns to detect human-specific drug–drug interactions.

We have described the maintenance of liver-specific drug metabolism functions in 3D hepatic microtissues, enabling early-stage screening of drug-induced liver injury and drug–drug interactions in primary hepatocytes. The ability to use primary hepatocytes as model cells carries the potential to predict diverse or idiosyncratic liver responses from individuals with varying risk factors such as age, gender, genetics, or underlying diseases.

Acknowledgments

The authors thank Lia Ingaharro (MIT) for performing hepatocyte isolations and general technical support, Heather Fleming (MIT) for editing this article, Kathleen Christine (MIT) for the mCherry J2-3T3 line, and Shengyong Ng (MIT) and Salman Khetani (Colorado State) for insightful discussions. They also thank MIT's Microsystems Technology Laboratories for microfabrication facilities, and Salil Desai (MIT) and Kartik Trehan (MIT) for fabrication assistance. The J2-3T3 fibroblast cell line was kindly provided by Howard Green (Harvard). This work was supported by grants from the National Institutes of Health (UH2 EB017103, R01 EB008396, and R01 DK85713) and, in part, by the Koch Institute Support (core) Grant P30-CA14051 from the National Cancer Institute. R.E.S. is supported by the American Gastroenterological Association Research Scholar Fellowship. C.Y.L. is supported by the National Science Foundation Graduate Research Fellowship Program (1122374). S.N.B. is an HHMI Investigator. The authors wish to dedicate this article to the memory of Officer Sean Collier, for his caring service to the MIT community and for his sacrifice.

Disclosure Statement

No competing financial interests exist.

References

1. Wilkening, S., Stahl, F., and Bader, A. Comparison of primary human hepatocytes and hepatoma cell line Hepg2 with regard to their biotransformation properties. Drug Metab Dispos **31,** 1035, 2003.
2. Phillips, A., Hood, S.R., Gibson, G.G., and Plant, N.J. Impact of transcription factor profile and chromatin conformation on human hepatocyte CYP3A gene expression. Drug Metab Dispos **33,** 233, 2005.
3. Gerets, H.H., Tilmant, K., Gerin, B., Chanteux, H., Depelchin, B.O., Dhalluin, S., *et al.* Characterization of primary human hepatocytes, HepG2 cells, and HepaRG cells at the mRNA level and CYP activity in response to inducers and their predictivity for the detection of human hepatotoxins. Cell Biol Toxicol **28,** 69, 2012.
4. Fraczek, J., Bolleyn, J., Vanhaecke, T., Rogiers, V., and Vinken, M. Primary hepatocyte cultures for pharmacotoxicological studies: at the busy crossroad of various anti-dedifferentiation strategies. Arch Toxicol **87,** 577, 2013.
5. LeCluyse, E.L. Human hepatocyte culture systems for the *in vitro* evaluation of cytochrome P450 expression and regulation. Eur J Pharm Sci **13,** 343, 2001.
6. Guillouzo, A. Liver cell models in *in vitro* toxicology. Environ Health Perspect **106 Suppl 2,** 511, 1998.
7. Tong, J.Z., Bernard, O., and Alvarez, F. Long-term culture of rat-liver cell spheroids in hormonally defined media. Exp Cell Res **189,** 87, 1990.
8. Hamilton, G., Westmoreland, C., and George, E. Effects of medium composition on the morphology and function of rat hepatocytes cultured as spheroids and monolayers. In Vitro Cell Dev Biol Anim **37,** 656, 2001.
9. Dvir-Ginzberg, M., Elkayam, T., Aflalo, E.D., Agbaria, R., and Cohen, S. Ultrastructural and functional investigations of adult hepatocyte spheroids during *in vitro* cultivation. Tissue Eng **10,** 1806, 2004.
10. Dunn, J.C., Tompkins, R.G., and Yarmush, M.L. Long-term *in vitro* function of adult hepatocytes in a collagen sandwich configuration. Biotechnol Prog **7,** 237, 1991.
11. Richert, L., Binda, D., Hamilton, G., Viollon-Abadie, C., Alexandre, E., Bigot-Lasserre, D., *et al.* Evaluation of the effect of culture configuration on morphology, survival time, antioxidant status and metabolic capacities of cultured rat hepatocytes. Toxicol In Vitro **16,** 89, 2002.
12. Glicklis, R., Shapiro, L., Agbaria, R., Merchuk, J.C., and Cohen, S. Hepatocyte behavior within three-dimensional porous alginate scaffolds. Biotechnol Bioeng **67,** 344, 2000.
13. Kaufmann, P.M., Heimrath, S., Kim, B.S., and Mooney, D.J. Highly porous polymer matrices as a three-dimensional culture system for hepatocytes. Cell Transplant **6,** 463, 1997.
14. Underhill, G.H., Chen, A.A., Albrecht, D.R., and Bhatia, S.N. Assessment of hepatocellular function within PEG hydrogels. Biomaterials **28,** 256, 2007.
15. Chen, A.A., Thomas, D.K., Ong, L.L., Schwartz, R.E., Golub, T.R., and Bhatia, S.N. Humanized mice with ectopic artificial liver tissues. Proc Natl Acad Sci U S A **108,** 11842, 2011.
16. Nishikawa, Y., Tokusashi, Y., Kadohama, T., Nishimori, H., and Ogawa, K. Hepatocytic cells form bile duct-like structures within a three-dimensional collagen gel matrix. Exp Cell Res **223,** 357, 1996.
17. Glicklis, R., Merchuk, J.C., and Cohen, S. Modeling mass transfer in hepatocyte spheroids via cell viability, spheroid size, and hepatocellular functions. Biotechnol Bioeng **86,** 672, 2004.
18. Tostoes, R.M., Leite, S.B., Miranda, J.P., Sousa, M., Wang, D.I., Carrondo, M.J., *et al.* Perfusion of 3D encapsulated hepatocytes—a synergistic effect enhancing long-term functionality in bioreactors. Biotechnol Bioeng **108,** 41, 2011.
19. Wilson, J.L., and McDevitt, T.C. Stem cell microencapsulation for phenotypic control, bioprocessing, and transplantation. Biotechnol Bioeng **110,** 667, 2013.
20. Curcio, E., Salerno, S., Barbieri, G., De Bartolo, L., Drioli, E., and Bader, A. Mass transfer and metabolic reactions in hepatocyte spheroids cultured in rotating wall gas-permeable membrane system. Biomaterials **28,** 5487, 2007.
21. Tumarkin, E., Tzadu, L., Csaszar, E., Seo, M., Zhang, H., Lee, A., *et al.* High-throughput combinatorial cell co-culture using microfluidics. Integr Biol (Camb) **3,** 653, 2011.
22. Li, C.Y., Wood, D.K., Huang, J.H., and Bhatia, S.N. Flow-based pipeline for systematic modulation and analysis of 3D tumor microenvironments. Lab Chip. **13,** 1969, 2013.
23. Burdick, J.A., and Anseth, K.S. Photoencapsulation of osteoblasts in injectable RGD-modified PEG hydrogels for bone tissue engineering. Biomaterials **23,** 4315, 2002.
24. Moon, J.J., Hahn, M.S., Kim, I., Nsiah, B.A., and West, J.L. Micropatterning of poly(ethylene glycol) diacrylate hydrogels

with biomolecules to regulate and guide endothelial morphogenesis. Tissue Eng Part A **15,** 579, 2009.
25. Lin, C.C., and Anseth, K.S. Cell-cell communication mimicry with poly(ethylene glycol) hydrogels for enhancing beta-cell function. Proc Natl Acad Sci U S A **108,** 6380, 2011.
26. DeLong, S.A., Mann, B.K., and West, J.L. Scaffolds modified with tethered growth factors to influence smooth muscle cell behavior. FASEB J **16,** A36 2002.
27. Kumachev, A., Greener, J., Tumarkin, E., Eiser, E., Zandstra, P.W., and Kumacheva, E. High-throughput generation of hydrogel microbeads with varying elasticity for cell encapsulation. Biomaterials **32,** 1477, 2011.
28. Li, C.Y., Wood, D.K., Hsu, C.M., and Bhatia, S.N. DNA-templated assembly of droplet-derived PEG microtissues. Lab Chip **11,** 2967, 2011.
29. Chen, A.A., Underhill, G.H., and Bhatia, S.N. Multiplexed, high-throughput analysis of 3D microtissue suspensions. Integr Biol (Camb) **2,** 517, 2010.
30. Anderson, S.B., Lin, C.C., Kuntzler, D.V., and Anseth, K.S. The performance of human mesenchymal stem cells encapsulated in cell-degradable polymer-peptide hydrogels. Biomaterials **32,** 3564, 2011.
31. Yanagawa, F., Kaji, H., Jang, Y.H., Bae, H., Yanan, D., Fukuda, J., *et al.* Directed assembly of cell-laden microgels for building porous three-dimensional tissue constructs. J Biomed Mater Res Part A 2011 [Epub ahead of print]; DOI: 10.1002/jbm.a.33034.
32. Zamanian, B., Masaeli, M., Nichol, J.W., Khabiry, M., Hancock, M.J., Bae, H., *et al.* Interface-directed self-assembly of cell-laden microgels. Small **6,** 937, 2010.
33. Khan, O.F., and Sefton, M.V. Perfusion and characterization of an endothelial cell-seeded modular tissue engineered construct formed in a microfluidic remodeling chamber. Biomaterials **31,** 8254, 2010.
34. McGuigan, A.P., and Sefton, M.V. Vascularized organoid engineered by modular assembly enables blood perfusion. Proc Natl Acad Sci U S A **103,** 11461, 2006.
35. Bruzewicz, D.A., McGuigan, A.P., and Whitesides, G.M. Fabrication of a modular tissue construct in a microfluidic chip. Lab Chip **8,** 663, 2008.
36. Seglen, P.O. Preparation of isolated rat liver cells. Methods Cell Biol **13,** 29, 1976.
37. Liu Tsang, V., Chen, A.A., Cho, L.M., Jadin, K.D., Sah, R.L., DeLong, S., *et al.* Fabrication of 3D hepatic tissues by additive photopatterning of cellular hydrogels. FASEB J **21,** 790, 2007.
38. Hui, E.E., and Bhatia, S.N. Micromechanical control of cell-cell interactions. Proc Natl Acad Sci U S A **104,** 5722, 2007.
39. Khetani, S.R., and Bhatia, S.N. Microscale culture of human liver cells for drug development. Nat Biotechnol **26,** 120, 2008.
40. Bhatia, S.N., Balis, U.J., Yarmush, M.L., and Toner, M. Probing heterotypic cell interactions: hepatocyte function in microfabricated co-cultures. J Biomater Sci Poly Ed **9,** 1137, 1998.
41. Lu, H.F., Chua, K.N., Zhang, P.C., Lim, W.S., Ramakrishna, S., Leong, K.W., *et al.* Three-dimensional co-culture of rat hepatocyte spheroids and NIH/3T3 fibroblasts enhances hepatocyte functional maintenance. Acta Biomater **1,** 399, 2005.
42. Cruise, G.M., Scharp, D.S., and Hubbell, J.A. Characterization of permeability and network structure of interfacially photopolymerized poly(ethylene glycol) diacrylate hydrogels. Biomaterials **19,** 1287, 1998.
43. Jabbari, E. Bioconjugation of hydrogels for tissue engineering. Curr Opin Biotechnol **22,** 655, 2011.
44. Hume, P.S., and Anseth, K.S. Polymerizable superoxide dismutase mimetic protects cells encapsulated in poly(ethylene glycol) hydrogels from reactive oxygen species-mediated damage. J Biomed Mater Res Part A **99A,** 29, 2011.
45. Stevens, K.R., Ungrin, M.D., Schwartz, R.E., Carvalho, B., Christine, K.S., Chaturvedi, R., *et al.* InVERT molding for scalable control of tissue microarchitecture. Nat Commun **4,** 1847, 2013.
46. Lemaire, G., Delescluse, C., Pralavorio, M., Ledirac, N., Lesca, P., and Rahmani, R. The role of protein tyrosine kinases in CYP1A1 induction by omeprazole and thiabendazole in rat hepatocytes. Life Sci **74,** 2265, 2004.
47. Lu, C., and Li, A.P. Species comparison in P450 induction: effects of dexamethasone, omeprazole, and rifampin on P450 isoforms 1A and 3A in primary cultured hepatocytes from man, Sprague-Dawley rat, minipig, and beagle dog. Chem Biol Interact **134,** 271, 2001.
48. Martignoni, M., Groothuis, G.M.M., and de Kanter, R. Species differences between mouse, rat, dog, monkey and human CYP-mediated drug metabolism, inhibition and induction. Expert Opin Drug Met **2,** 875, 2006.
49. Chen, Y.P., Ferguson, S.S., Negishi, M., and Goldstein, J.A. Induction of human CYP2C9 by rifampicin, hyperforin, and phenobarbital is mediated by the pregnane X receptor. J Pharmacol Exp Ther **308,** 495, 2004.
50. Patten, C.J., Thomas, P.E., Guy, R.L., Lee, M., Gonzalez, F.J., Guengerich, F.P., *et al.* Cytochrome P450 enzymes involved in acetaminophen activation by rat and human liver microsomes and their kinetics. Chem Res Toxicol **6,** 511, 1993.
51. McCloskey, P., Edwards, R.J., Tootle, R., Selden, C., Roberts, E., and Hodgson, H.J. Resistance of three immortalized human hepatocyte cell lines to acetaminophen and N-acetyl-p-benzoquinoneimine toxicity. J Hepatol **31,** 841, 1999.
52. Kaplowitz, N. Idiosyncratic drug hepatotoxicity. Nat Rev Drug Discov **4,** 489, 2005.
53. Schutte, M., Fox, B., Baradez, M.O., Devonshire, A., Minguez, J., Bokhari, M., *et al.* Rat primary hepatocytes show enhanced performance and sensitivity to acetaminophen during three-dimensional culture on a polystyrene scaffold designed for routine use. Assay Drug Dev Technol **9,** 475, 2011.
54. Shih, H., Pickwell, G.V., Guenette, D.K., Bilir, B., and Quattrochi, L.C. Species differences in hepatocyte induction of CYP1A1 and CYP1A2 by omeprazole. Hum Exp Toxicol **18,** 95, 1999.
55. Sargent, C.Y., Berguig, G.Y., Kinney, M.A., Hiatt, L.A., Carpenedo, R.L., Berson, R.E., *et al.* Hydrodynamic modulation of embryonic stem cell differentiation by rotary orbital suspension culture. Biotechnol Bioeng **105,** 611, 2010.
56. Landry, J., Bernier, D., Ouellet, C., Goyette, R., and Marceau, N. Spheroidal aggregate culture of rat liver cells: histotypic reorganization, biomatrix deposition, and maintenance of functional activities. J Cell Biol **101,** 914, 1985.
57. Brophy, C.M., Luebke-Wheeler, J.L., Amiot, B.P., Khan, H., Remmel, R.P., Rinaldo, P., *et al.* Rat hepatocyte spheroids formed by rocked technique maintain differentiated hepatocyte gene expression and function. Hepatology **49,** 578, 2009.

58. Lin, R.-Z., and Chang, H.-Y. Recent advances in three-dimensional multicellular spheroid culture for biomedical research. Biotechnol J **3,** 1172, 2008.
59. Drewitz, M., Helbling, M., Fried, N., Bieri, M., Moritz, W., Lichtenberg, J., *et al.* Towards automated production and drug sensitivity testing using scaffold-free spherical tumor microtissues. Biotechnol J **6,** 1488, 2011.
60. Ungrin, M.D., Joshi, C., Nica, A., Bauwens, C., and Zandstra, P.W. Reproducible, ultra high-throughput formation of multicellular organization from single cell suspension-derived human embryonic stem cell aggregates. PLoS One **3,** e1565. 2008.
61. Ueno, K., Miyashita, A., Endoh, E., Takezawa, T., Yamazaki, M., Mori, Y., *et al.* Formation of multicellular spheroids composed of rat hepatocytes. Res Commun Chem Pathol Pharmacol **77,** 107, 1992.
62. Pinkse, G.G.M., Jiawan-Lalai, R., Bruijn, J.A., and de Heer, E. RGD peptides confer survival to hepatocytes via the beta 1-integrin-ILK-pAkt pathway. J Hepatol **42,** 87, 2005.
63. Maheshwari, G., Brown, G., Lauffenburger, D.A., Wells, A., and Griffith, L.G. Cell adhesion and motility depend on nanoscale RGD clustering. J Cell Sci **113,** 1677, 2000.
64. Schwartz, M.A., and Ginsberg, M.H. Networks and crosstalk: integrin signalling spreads. Nat Cell Biol **4,** E65, 2002.
65. Wang, F., Weaver, V.M., Petersen, O.W., Larabell, C.A., Dedhar, S., Briand, P., *et al.* Reciprocal interactions between beta1-integrin and epidermal growth factor receptor in three-dimensional basement membrane breast cultures: a different perspective in epithelial biology. Proc Natl Acad Sci U S A **95,** 14821, 1998.
66. Powers, M.J., and Griffith-Cima, L. Motility behavior of hepatocytes on extracellular matrix substrata during aggregation. Biotechnol Bioeng **50,** 392, 1996.
67. Pinkse, G.G.M., Voorhoeve, M.P., Noteborn, M., Terpstra, O.T., Bruijn, J.A., and de Heer, E. Hepatocyte survival depends on beta 1-integrin-mediated attachment of hepatocytes to hepatic extracellular matrix. Liver Int **24,** 218, 2004.
68. Xu, J.J., Henstock, P.V., Dunn, M.C., Smith, A.R., Chabot, J.R., and de Graaf, D. Cellular imaging predictions of clinical drug-induced liver injury. Toxicol Sci **105,** 97, 2008.
69. Ukairo, O., Kanchagar, C., Moore, A., Shi JLN, Gaffney, J., Aoyama, S., *et al.* Long-term stability of primary rat hepatocytes in micropatterned cocultures. J Biochem Mol Toxicol **27,** 204, 2013.

Address correspondence to:
Sangeeta N. Bhatia, PhD
Electrical Engineering and Computer Science
Massachusetts Institute of Technology
500 Main St. Bldg 76-453
Cambridge, MA 02142

E-mail: sbhatia@mit.edu

Received: October 29, 2013
Accepted: January 31, 2014
Online Publication Date: April 25, 2014